STM JOURNALS

Journal of
Polymer & Composites

ISSN: 2321-2810 (Online)
ISSN: 2321-8525 (Print)
Volume 13, Special Issue 1, 2025
DOI (Journal): 10.37591/JoPC

https://journals.stmjournals.com/jopc

Review JoPC

Experimental and Numerical Studies on Radial Tensile Strength of Composite Rotor

Gopi Erulan[1,*], Gowthaman Swaminathan [2]

Abstract

This paper describes the experimental and numerical studies on the radial tensile strength (RTS) of composite rotor. Carbon/epoxy composite rotors were fabricated using a filament winding process and their radial tensile strength was determined by diametric tensile testing of composite C-rings. The radial tensile strength of the composite rotor was measured as ~ 22 MPa and the failure was found to occur circumferentially symmetric about the horizontal plane of the C-ring. It also occurred at the same radial positions on both the front and back axial faces of the sample. Unidirectional carbon/epoxy composite panels were also fabricated using a flat mandrel in the filament winding process and their tensile properties were determined. Based on the experimental results and by applying the Rule of Mixtures, the inherent moduli of the composite rotor were determined. Then, numerical analysis was performed to evaluate and verify the RTS of the composite rotor. The studies showed that the RTS from both the experiments and numerical analysis matched well. Also, in numerical analysis, the interlaminar shear stress was negligible and this implied that the C-ring failed purely by radial stress. It was also observed that the maximum radial tensile stress occurred at the mid-region of the radial thickness, and this also matched well with the experiments.

Keywords: Polymer composite rotor, mechanical properties, carbon fiber, epoxy, radial tensile strength, c-ring test, finite element analysis

INTRODUCTION

A filament wound, fibre-reinforced composite rotors are used in several applications because of their high specific properties. For example, thick composite rotors are used in flywheels due to their high energy storage capacity. However, thick composite rotors are subjected to large radial tensile stresses and the radial tensile strength becomes the critical design parameter in thick composite rotors. Different test methods like diametric tension of a full ring [1]. diametric tension of a C-ring [2,3]. axial tension of a full ring [2]. through-thickness tension of a thick laminated composite [4] and uni-axial tension of coupon machined from thick rotor [5-7]. have been used to measure the RTS of thick composites. For example, Wu et al [1]. measured the RTS using the diametric tension of the full ring. However, it was noted that residual stresses must be accounted for this type of test. Tensile coupons also presented a few problems, wherein the measured radial strength was found to be not accurate because of stress concentrations near the grips. Alternatively, measurement of radial strength using a C-ring sample has been found to be very effective as it eliminates the above-mentioned problems. Researchers have also performed C-ring tests with few modifications so as to ensure the failure of C-rings only by radial stress [8-11].

***Author for Correspondence**
Gopi Erulan

[1]Research Scholar, Department of Mechanical Engineering, Indian Institute of Information Technology Design and Manufacturing Kancheepuram, Chennai, Tamil Nadu, India
[2]Faculty, Department of Mechanical Engineering, Indian Institute of Information Technology Design and Manufacturing Kancheepuram, Chennai, Tamil Nadu, India

Received Date: June 13, 2024
Accepted Date: July 25, 2024
Published Date: December 12, 2024

Citation: Gopi Erulan, Gowthaman Swaminathan. Experimental and Numerical Studies on Radial Tensile Strength of Composite Rotor. Journal of Polymer & Composites. 2025; 13(Special Issue 1): S985–S996p.

The present study aimed to evaluate and verify the RTS of filament-wound composite rotor

fabricated using Tansome carbon fiber (H2550-6k) and epoxy resin. The composite rotors made using Tansome carbon fiber (H2550-6k) will be used in future for designing composite flywheels and the property data for this material system is currently not available in the literature. In the present study, the RTS was measured using a diametrical tensile test of filament wound C-ring. Care was taken to ensure that the interlaminar shear stresses were negligible. The basic composite laminate properties were determined using coupons cut from filament-wound composite panels. Then, a numerical study was performed to determine the RTS of the C-ring and compare it with experimental results.

EXPERIMENTS

Materials

Tansome carbon fiber (H2550-6k) from Hyosung Advanced Materials, Korea was used as a continuous reinforcement for the fabrication of composite rotors and panels. The fibers were procured from Jalark Carbon Products, Vadodara, India. A DGEBA based low-viscosity epoxy resin (Araldite GY 257) together with an amine-based curing agent (Aradur 847) was used as the resin system. Both the resin and hardener were procured from Javanthee Enterprises, Chennai, India. The epoxy equivalent weight of resin was 182-192 g/Eq and the amine hydrogen equivalent weight of hardener (curing agent) was 75 g/Eq. As such, a resinhardener mix ratio of 100 : 40 and a curing cycle of 24 hours at room temperature was used in the fabrication of resin and composites.

Fabrication

Epoxy resin samples

Epoxy resin samples were fabricated to determine the tensile properties. Epoxy resin and hardener were mixed homogeneously using a mechanical stirrer. The mixture was then degassed in a vacuum chamber. After degassing, the mixture was poured into the mold, which was made according to ASTM D 638 Type IV standard [12-14]. The resin samples were then de-molded after being allowed to cure for a duration of 24 hours at room temperature.

Unidirectional composite panels

Unidirectional carbon/epoxy composite panels were fabricated to determine the longitudinal tensile properties. Using Tansome carbon fiber (H2550-6k) and epoxy resin, the composite panels were prepared using the filament winding technique. The process consisted of the deposition of continuous filaments impregnated with resin onto a rotating flat mandrel. A constant tension in the filaments was created by passing the filament through a suspending roller attached to a dry weight of 400 g. The mandrel was rotated at a speed of 35 rpm. The entire carriage consisting of the resin bath and the guide ring was moved parallel to the mandrel axis at a suitable speed to have continuous winding of filaments along the axial direction. Using this procedure, composite panels of dimensions 250 x 60 x 1.5 mm were fabricated. Filament winding using flat mandrel and the filament wound composite panel is shown in Figure 1(a) and (b), respectively. The fiber volume fraction of the rotor was determined theoretically as well as experimentally (by matrix burn-off method) [15]. It was measured to be 0.48 in both methods.

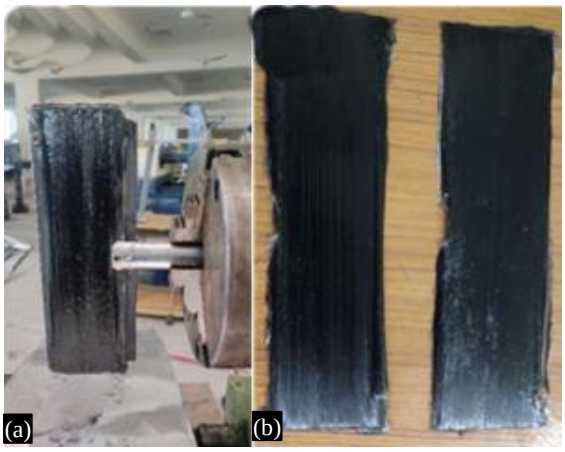

Figure 1. (a) Filament winding using flat mandrel and (b) filament wound composite panels.

Composite C-rings

Carbon/epoxy composite C-rings were fabricated to determine the RTS. Composite rotors of inner radius 47.7 mm, an outer radius of 57.7 mm and an axial height of 25 mm were fabricated using filament winding technique. Then, a 30 mm cut was made on the rotor using waterjet cutting to get C-shaped rings. The photograph of the filament wound composite rotor and the C-ring is shown in Figure 2(a) and (b), respectively. The fiber volume fraction of the rotor was determined theoretically as well as experimentally (by matrix burn-off method). It was measured to be 0.60 in both methods.

Mechanical Testing

Tensile testing of resin samples

Epoxy resin samples were tested according to ASTM D 638. The schematic of the epoxy sample for the tensile test is shown in Figure 3(a). Tensile tests were performed at a displacement speed of 1 mm/min with a Universal testing machine (UTM) equipped with a 50 kN load cell. The tensile strain was measured directly using an extensometer attached in the middle of the gauge length. Load-displacement data were recorded continuously until the failure of the samples. In total, five number of resin samples were tested.

Tensile testing of composite samples

Tensile testing of carbon composites was carried out as per the ASTM standard D 3039 [16,17]. The schematic of the composite sample for the tensile test is shown in Figure 3(b). Tensile samples of dimension 250 × 15 × 1.5 mm were cut from the fabricated composite panel. To ensure proper gripping during the testing, tabs made of glass/epoxy insulation material were attached to the composite samples. The tensile tests at a displacement speed of 1 mm/min were performed using UTM with a 400 kN load cell. Load-displacement data were recorded until the failure of the samples. The tensile strain was measured directly using an extensometer attached in the middle of the gauge length. In total, three number of composite samples were tested.

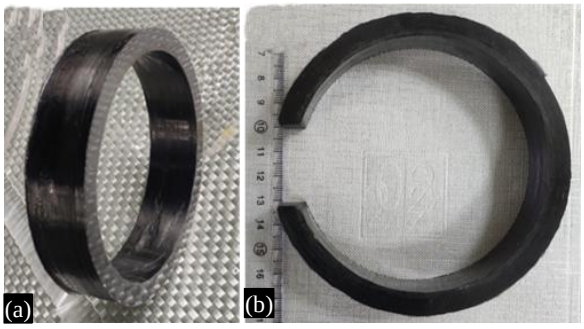

Figure 2. (a) Filament wound composite rotor and (b) composite c-ring.

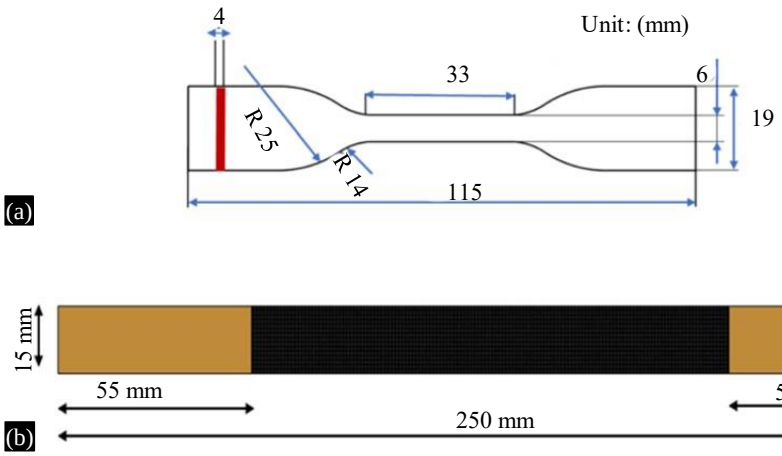

Figure 3. Schematic of tensile test samples of (a) resin and (b) composite.

Diametric tensile testing of composite c-rings

Diametric tensile testing of C-rings was carried out to determine the RTS of the composite rotors. The tests were performed using an Instron 3369 UTM with a 50 kN load cell. The C-ring samples were loaded onto the test equipment using a specially designed fixture as shown in Figure 4. The tests were conducted at a displacement speed of 1 mm/min and the load-displacement data were continuously recorded until the failure of the samples. In total, four number of samples were tested. The radial strength of the samples was calculated using the equation (1) given below.

$$\sigma_{r,max} = \frac{3PL}{2ht\sqrt{r_i r_o}} \quad (1)$$

where, P is the maximum load in N, L is loading arm distance i.e, ($r_i + t/2$) in mm, h is the axial height of the C-ring in mm, t is the radial thickness in mm, r_i is the inner radius of the C-ring in mm and r_o is the outer radius of the C-ring in mm [18].

NUMERICAL ANALYSIS

Numerical analysis was conducted to determine and verify the RTS of composite C-rings. Similar to that used in experiments, the composite C-ring was modeled with the same dimensions and boundary conditions using ANSYS 19R. The composite properties (E_X, E_Y and E_m) as determined from the experiments were used as the input material properties. A cylindrical coordinate system was used to define the material properties and the C-ring model was discretized by quadrilateral finite elements with an element size of 1 mm. The model of the C-ring, along with boundary conditions is shown in Figure 5. To simulate the experiments, the lower loading rod was fixed in all directions. The upper loading rod was allowed to undergo displacement only in the positive Y-direction. The peak load corresponding to the failure of the sample, as obtained from the C-ring test was given as the input tensile load. This tensile load was applied as a line pressure along the axial length of the upper loading rod in the positive Y-direction.

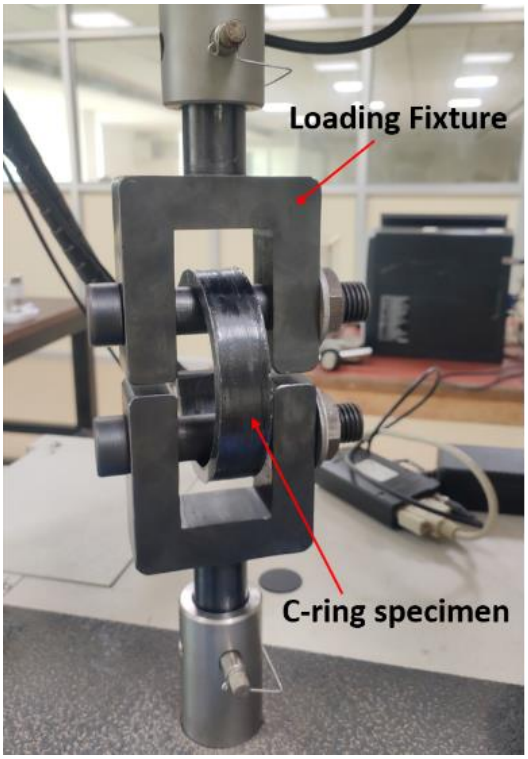

Figure 4. Diametric tensile test setup.

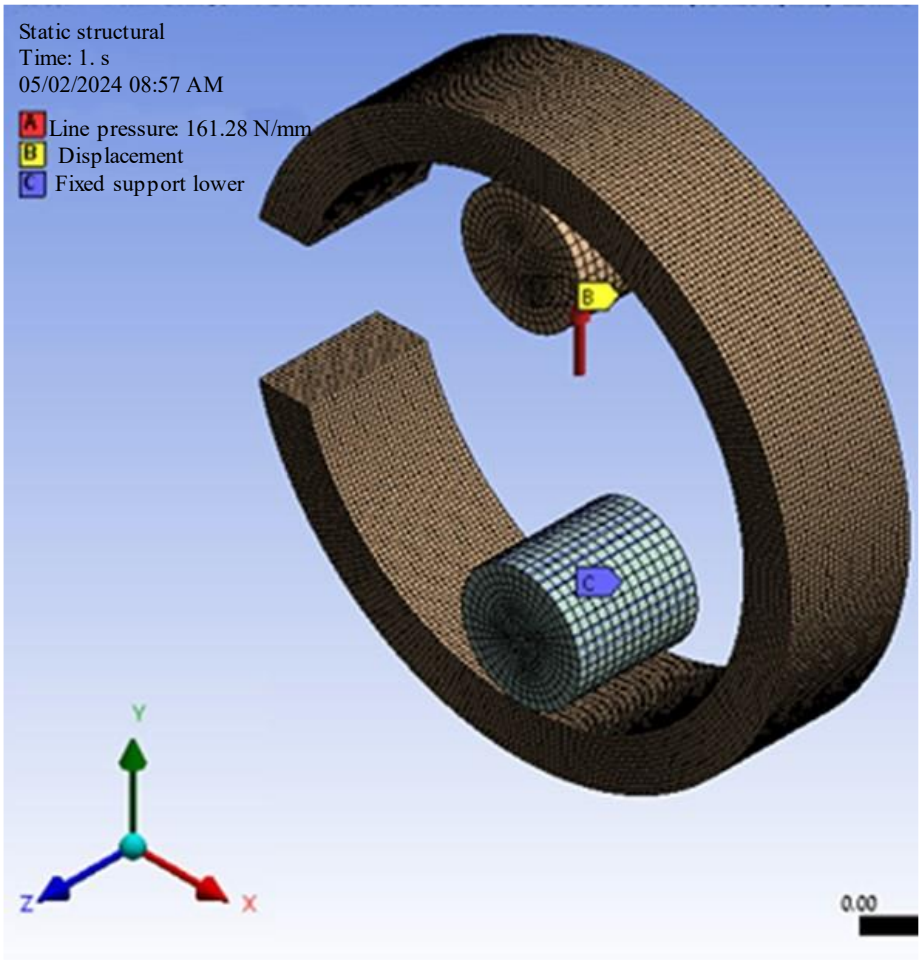

Figure 5. C-ring model with boundary conditions.

RESULTS AND DISCUSSIONS

Figure 6 shows the stress-strain behaviour of all the epoxy resin samples. Table 1 lists the tensile properties of all the epoxy resin samples along with average and standard deviation (SD). The average tensile modulus and average tensile strength of epoxy resin was measured to be 2.7 GPa and 37 MPa, respectively. Figure 7(a) shows the load-displacement behaviour of all the filament-wound carbon/epoxy composite samples and Figure 7(b) shows the stress-strain behaviour of all the carbon/epoxy composite samples. The stress-strain behaviour was shown only until around 0.25 to 0.4% strain, beyond which the extensometer went off-scale. The tensile properties of all the composite samples, along with the average and SD, were listed in Table 1. The average tensile modulus and average tensile strength of the composite was measured to be 123 GPa and 1349 MPa, respectively. By taking into account of fiber volume fraction (V_f = 0.48), the Young's modulus and tensile strength of Tansome carbon fiber (H2550-6k) was then calculated using the Rule of Mixtures (ROM) [19]. The Young's modulus and tensile strength of the carbon fiber was calculated to be 253 GPa and 2779 MPa, respectively. The calculated Young's modulus (253 GPa) of the carbon fiber matched closely with Young's modulus (250 GPa) in the datasheet [20]. However, the calculated fiber strength (2779 MPa) of the carbon fiber did not match the strength of the fiber (5516 MPa) in the datasheet. This could be attributed to the use of different lengths of carbon fibers to measure their properties. Shorter-length single fibers are commonly used to measure the strength and the strength measured by this method has been listed in the datasheet. However, in the present study, a cluster of longer-length fibers were used to fabricate the composite and then the strength of the fiber was calculated using ROM. This measured strength was lower than that reported in the datasheet. This could be attributed to the inherent statistical distribution of flaws and more number of flaws along the longer length of fibers [21-23]. As mentioned previously, the fiber volume fraction of filament wound composite rotors was 0.6. In order to calculate

the composite properties corresponding to V_f = 0.6, the properties of carbon fiber (E_f = 250 GPa) and resin (E_m = 2.7 GPa) were used in the ROM equations. As a result, corresponding to V_f = 0.6 for the composite rotor, Young's modulus was calculated to be 153.4 GPa and 6.64 GPa along and perpendicular to the fiber direction, respectively.

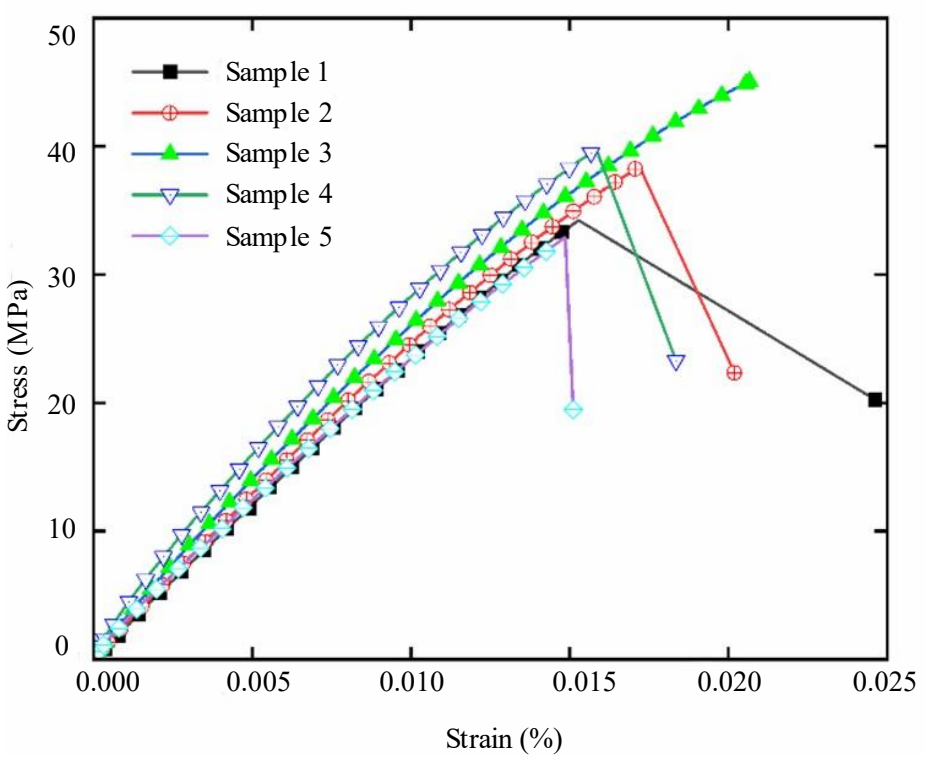

Figure 6. Tensile stress-strain behaviour of epoxy samples.

Table 1. Tensile Properties of Epoxy Resin and Carbon Composite.

Material	Sample No.	Young's modulus (GPa)	Failure stress (MPa)	Failure strain (%)
Epoxy Resin	1	2.4	34.2	0.024
	2	2.7	38.4	0.020
	3	2.9	44.2	0.028
	4	3.5	39.7	0.018
	5	2.6	32.8	0.015
	Average (SD)	2.7 (0.33)	37 (4.1)	0.021 (0.005)
Carbon/Epoxy Composite	1	120.8	1384.1	-
	2	124.6	1253.5	-
	3	124.4	1410.5	-
	Average (SD)	123.3 (2.1)	1349.3 (84.1)	-

Figure 8 shows the load-displacement behaviour of all the composite C-ring samples. Table 2 lists the radial tensile strength (RTS) of all the composite C-ring samples determined using Eq. 1 along with the average and SD. The average RTS of the filament wound composite rotor was found to be ~ 22 MPa. Figure 9 shows the failure of the C-ring sample under the diametrically opposite tension test. The failure coincided with the emergence of the initial circumferential crack, usually appearing at the mid-region of the radial thickness of the sample. Also, it occurred at the same radial region on the front and back axial face of the sample. It was observed that the crack occurred symmetric about the horizontal plane of the C-ring, but did not propagate to the complete length of the C-ring.

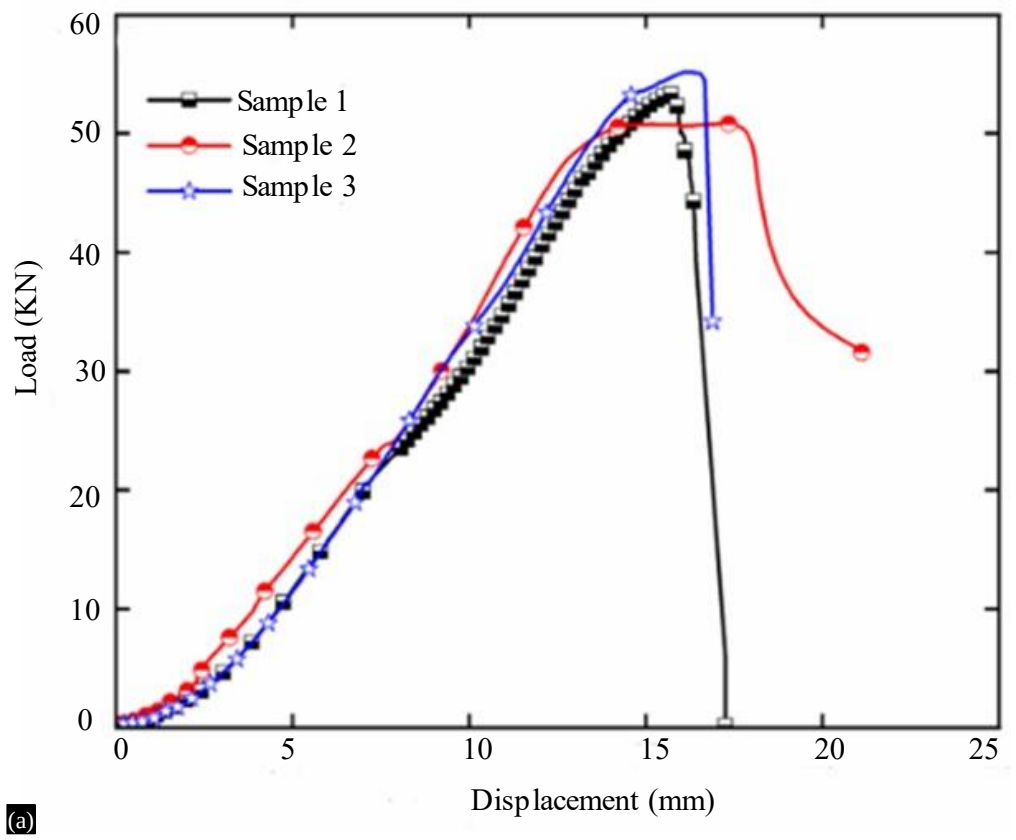

(a)

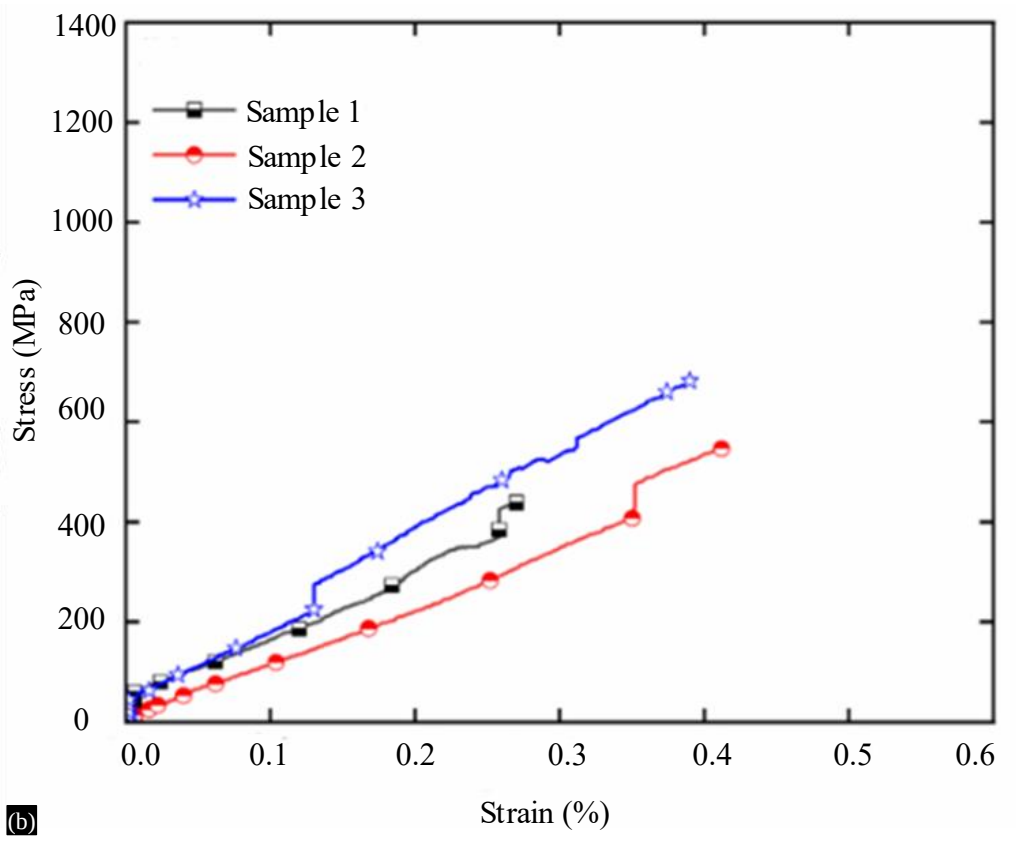

(b)

Figure 7. (a) Load-displacement and (b) stress-strain behaviour of composite samples under tensile test.

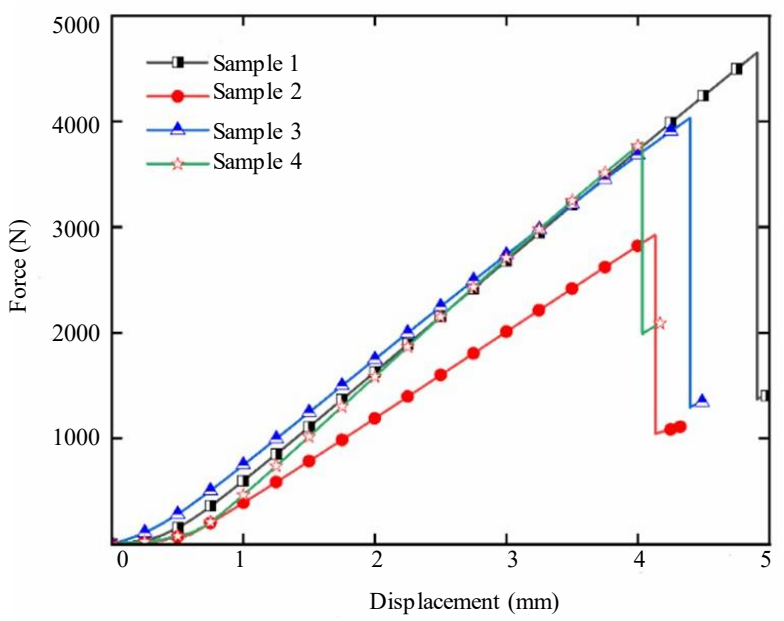

Figure 8. Load-displacement behaviour of c-ring samples under diametric tensile test.

Table 2. Radial Tensile Strength of Composite Rotors.

Sample #	Failure load (N)	Radial tensile strength (MPa)
1	4651.2	27.4
2	2925.1	18.2
3	4032.4	22.1
4	3800.3	20.8
Average (SD)		22.0 (3.8)

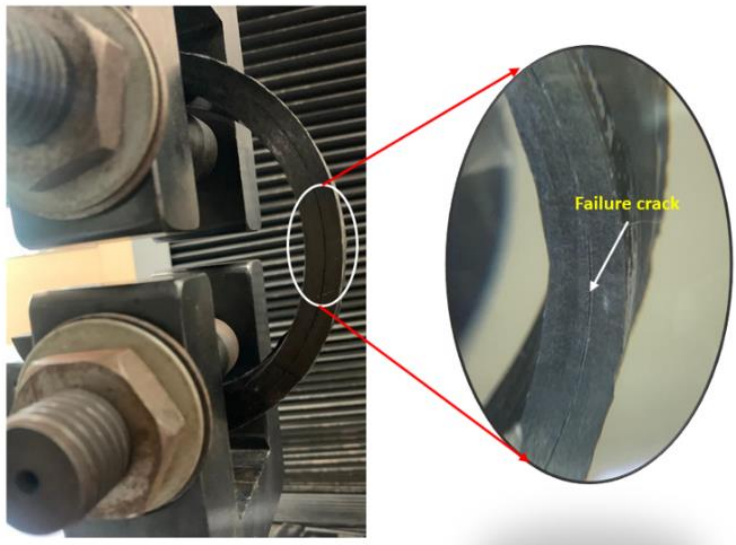

Figure 9: Failure of c-ring under diametric tensile test.

Numerical Analysis

Table 3 lists the input properties used in the numerical analysis of the C-ring test. For the loading rods, the structural steel property was assigned from the Ansys Material Library. The density of the composite rotor was calculated by using the mass and volume of the rotor. Corresponding to $V_f = 0.6$ for the C-ring, the previously calculated Young's modulus of 6.64 GPa (transverse), 153.4 GPa

(longitudinal) and 6.64 GPa (transverse) was taken as E_X, E_Y and E_Z, respectively. As per the literature, the Poisson's ratio (υ_{YZ}) of the composite was taken as υ_{YZ} = 0.295 [10]. Then, the other properties (υ_{XY}, υ_{XZ}, G_{XY}, G_{YZ} and G_{XZ}) were measured as per the equations available in the literature [19]. Corresponding to sample no 3 listed in Table 2, failure load 4032 N was applied as a line pressure on the bottom of the upper loading rod. This was equivalent to the line pressure of 161.28 N/mm. Fig. 10(a) shows the radial stress developed in the C-ring and loading rods. Figure 10(b) shows the variation of radial tensile stress and interlaminar shear stress along the radial thickness at 90˚ clockwise to the loading direction. The maximum RTS developed on the C-ring was ~ 22 MPa. This matched very well with the RTS that was measured using the experiment. The maximum radial stress was found to occur at 90˚ clockwise to the loading direction. It can be observed that the interlaminar shear stress was negligible and this implied that the C-ring failed purely by radial stress. It can also be observed that the maximum radial tensile stress occurred at the mid-region of the radial thickness. This matched well with the experiments, wherein the onset of circumferential failure occurred at the mid-region of the radial thickness.

Table 3. Material Properties For Numerical Analysis.

Properties of carbon/epoxy composite for (V_f = 0.6)	
Composite density (ρ_c)	1565 kg/m^3
Elastic modulus (E_X)	6.64 GPa
Elastic modulus (E_Y)	153.40 GPa
Elastic modulus (E_Z)	6.64 GPa
Poisson's Ratio XY (υ_{XY})	0.0129
Poisson's Ratio YZ (υ_{YZ})	0.295 [10]
Poisson's Ratio XZ (υ_{XZ})	0.4
Shear Modulus XY (G_{XY})	3.1 GPa
Shear Modulus YZ (G_{YZ})	3.1 GPa
Shear Modulus XZ (G_{XZ})	2.3 GPa
X - circumferential, Y & Z – radial and axial directions	

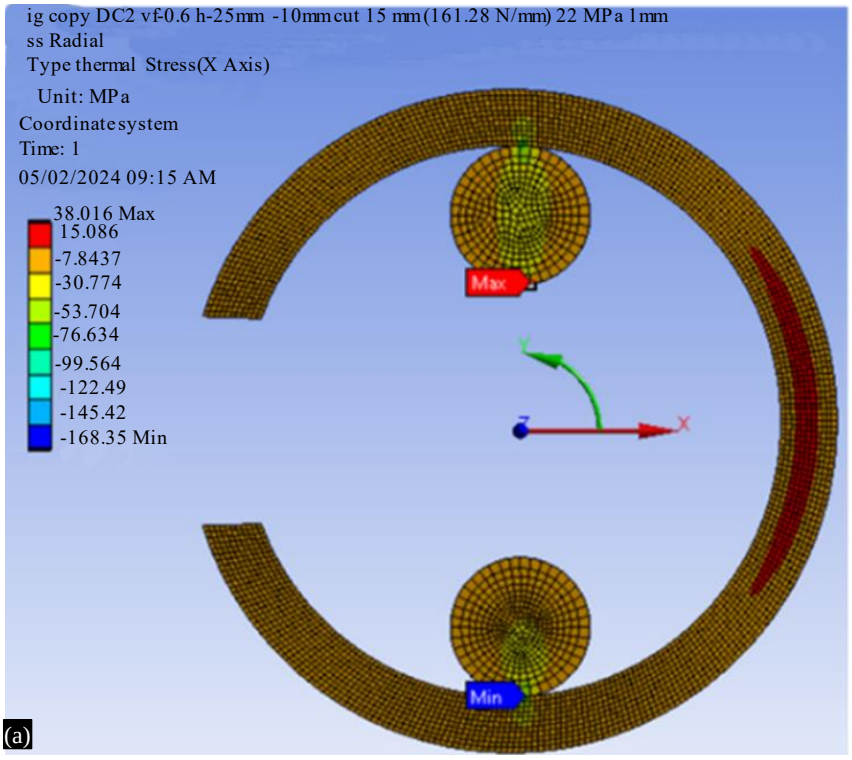

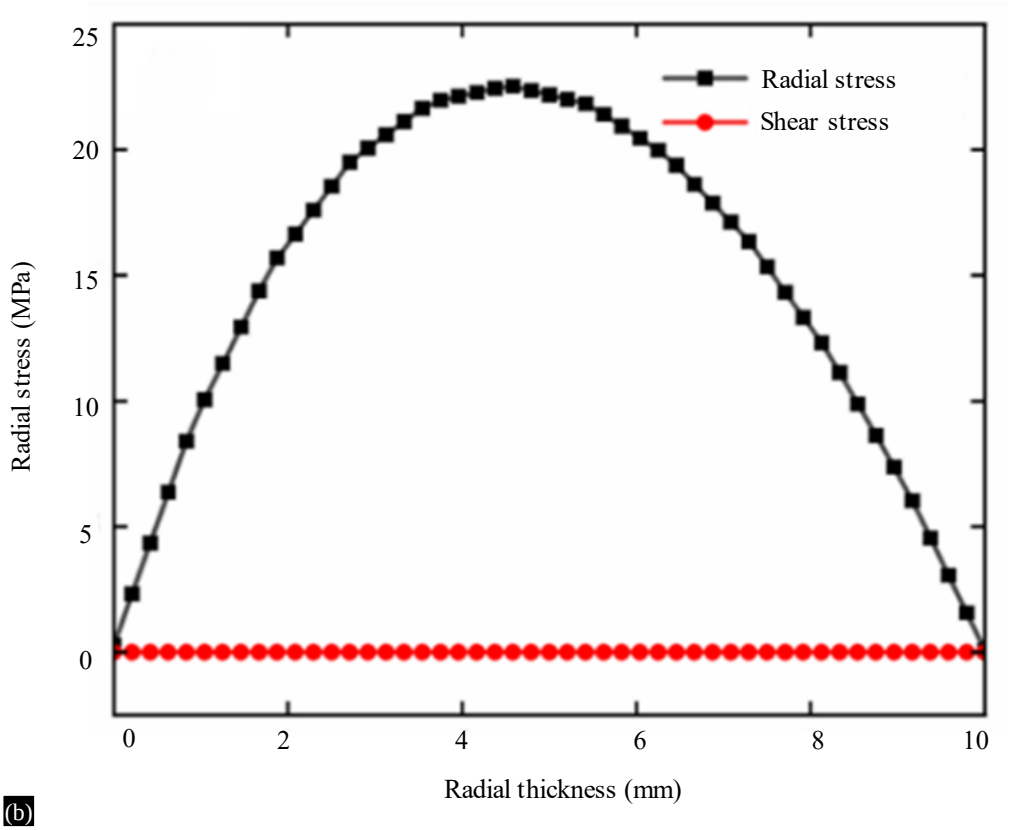

(b)

Figure 10. (a) Radial stress developed in c-ring and loading rods and (b) variation of radial stress and interlaminar shear stress along the radial thickness of c-ring.

CONCLUSIONS

Carbon/epoxy panels (with fiber volume fraction, V_f = 0.48) were fabricated using a flat mandrel in filament winding process. Carbon/epoxy composite rotors (with fiber volume fraction, V_f = 0.60) were fabricated using a cylindrical mandrel in filament winding process. Tensile testing of composite panels were conducted to determine the Young's modulus of composite along the fiber direction. Then, using the rule of mixtures, the Young's modulus of composite rotor was determined along and perpendicular to the fiber direction. The RTS of composite rotor was evaluated experimentally using diametric tensile testing of C-ring. Numerical analysis of composite C-ring test was also performed to determine and verify the RTS. The RTS of composite rotor that was determined from the experiments as well as the numerical analysis matched well. In the numerical analysis, the maximum radial stress occurred at the mid-region of the radial thickness. This also matched well with the experiments, wherein the onset of circumferential failure occurred at the mid-region of the radial thickness.

Declaration of Interest

The authors declare that there is no conflict of interest regarding the publication of this manuscript.

Acknowledgements

The authors acknowledge the funding support received from the Department of Science and Technology, India through grant # DST/TMD/MES/2K18/111.

REFERENCES

1. Wu YS, Longmuir AJ, Chandler HW, Gibson AG. Delamination of curved composite shells due to through-thickness tensile stresses. Plast. Rubber Compos 1993;19(1):39-46.
2. Tarnopolskii, Y.M. and Kincis, T. Static Test Methods for Composites. 1st ed. New York. Wiley & Sons, Incorporated, John;1985.

3. Rizov, V. and Ernst, L.J. On the Analysis of the Interlaminar Strain-Energy Release Rates in Ring-Fracture-Test Specimens. Compos Struct 2001;54: 331–334. https://doi.org/10.1016/S0263-8223(01)00106-4.
4. Koudela KL, Strait LH, Caiazzo AA, Gipple KL. Static and fatigue interlaminar tensile characterization of laminated composites. Composite Materials: Fatigue and Fracture (Sixth Volume) 1997 . ASTM International.
5. Orlet MW, Bakis CE. Viscoelastic characterization of high fiber content filament wound polyurethane matrix composites. Rubber Chem. Technol 1998;71(5):1042-58. https://doi.org/10.5254/1.3538509.
6. Gabrys CW, Bakis CE. Design and Manufacturing of Filament Wound Elastomeric Matrix Composite Flywheels. J. Reinf. Plast. Compos 1997;16(6):488-502. https://doi.org/10.1177/073168449701600601.
7. Ha SK, Jeong JY. Effects of winding angles on through-thickness properties and residual strains of thick filament wound composite rings. Compos. Sci. Technol 2005;65(1):27-35. https://doi.org/10.1016/j.compscitech.2004.05.019.
8. Portnov, G.G., Mungalov, D.D. & Barinov, I.N. Resistance of composite flywheel rim to radial tensile stresses from centrifugal forces based on results of pure bending of a rim segment. Mech Compos Mater 1994; 29:392–396. https://doi.org/10.1007/BF00617165.
9. Arnautov AK, Zhmud' NP. Experimental evaluation of the effect of the structure of composite rings on their properties in the radial direction. Mech. Compos. Mater. 2002;38:505-14. https://doi.org/10.1023/A:1021774525146.
10. Sharma A, Bakis CE. Analysis of Elastic Stresses in Thick, Polar–Orthotropic, C-Shaped Rings. J. Compos. Mater 2004;38(18):1619-38. https://doi.org/10.1177/0021998304043888.
11. Sharma A, Bakis CE. C-shape specimen for tensile radial strength of thick, filament-wound rings. J. Compos. Mater 2006;40(2):97-117. https://doi.org/10.1177/0021998305053505.
12. ASTM D638-14 (2014) Standard Test Method for Tensile Properties of Plastics. ASTM International, West Conshohocken. DOI: 10.1520/D0638-14.
13. Palanisamy S, Kalimuthu M, Azeez A, Palaniappan M, Dharmalingam S, Nagarajan R, Santulli C. Wear Properties and Post-Moisture Absorption Mechanical Behavior of Kenaf/Banana-Fiber-Reinforced Epoxy Composites. *Fibers*. 2022; 10(4):32. https://doi.org/10.3390/fib10040032.
14. Sumesh, K. R., Palanisamy, S., Khan, T., Ajithram, A., and Ahmed, O. S. (2024). Mechanical, morphological and wear resistance of natural fiber / glass fiber-based polymer composites. BioResources 2019:(2), 3271-3289. https://doi.org/10.15376/biores.19.2.3271-3289.
15. ASTM D3171–15, Standard Test Methods for Constituent Content of Composite Materials, ASTM International, West Conshohocken, PA 2015.
16. ASTM D3039/D3039M-00 (2000) Standard Test Method for Tensile Properties of Polymer Matrix Composite Materials. ASTM International, West Conshohocken, PA. DOI: 10.1520/D3039_D3039M-17.
17. Karuppiah G, Kuttalam KC, Palaniappan M, Santulli C, Palanisamy S. Multiobjective Optimization of Fabrication Parameters of Jute Fiber/Polyester Composites with Egg Shell Powder and Nanoclay Filler. Molecules. 2020; 25(23):5579. https://doi.org/10.3390/molecules25235579.
18. Kedward KT, Wilson RS, McLean SK. Flexure of simply curved composite shapes. Composites. 1989;20(6):527-36. https://doi.org/10.1016/0010-4361(89)90911-7.
19. Wang CH. Investigation on Metal-Composite Hybrid Flywheels using Finite Element Method [PhD thesis]. The University of Texas at Arlington;2017. Available from: https://mavmatrix.uta.edu/cgi/viewcontent.cgi?params=/context/mechaerospace_theses/article/1085/type/native/&path_info=. (Online Thesis)
20. Fiber data sheet.2017. Available from: https://hyosungusa.com/files/advanced/tansome_catalog_2017.pdf
21. Fidelis ME, Pereira TV, Gomes OD, de Andrade Silva F, Toledo Filho RD. The effect of fiber morphology on the tensile strength of natural fibers. J Mater Res Technol. 2013:149-57. https://doi.org/10.1016/j.jmrt.2013.02.003.

22. Prasannakumar I, Preetamkumar MM, Sudhir K. Axial tensile testing of single fibers. Mod Mech Eng. 2012;2:151-6. DOI: 10.4236/mme.2012.24020
23. Gowthaman S, Sankar CG, Chandrakumar P. Evaluation of tensile properties of natural silk and coir fibers. In: Innovative Design and Development Practices in Aerospace and Automotive Engineering: I-DAD, 2016 February 22-24, Chennai, India. Singapore: Springer; 2017. 393-9p.

